GEOPHYSICAL RESEARCH LETTERS, VOL. 23, NO. 5, PAGES 571-574, MARCH 1, 1996

High Altitude Discharges and Gamma-Ray Flashes: A Manifestation of Runaway Air Breakdown

Yuri Taranenko and Robert Roussel-Dupré

NIS-1, MS-D466, LANL, Los Alamos, NM

Abstract. γ-ray flashes of atmospheric origin as well as blue jets and red sprites are naturally explained by high-altitude discharges produced by runaway air breakdown. We present the first detailed model of the development of upward propagating discharges and compute optical and γ-ray emissions that are in excellent agreement with observations. According to our theory, such discharges represent the first known manifestation of runaway air breakdown, a fundamental new process in plasma physics.

Introduction

The origins of mysterious γ-ray flashes [*Fishman et al.*, 1994] of atmospheric origin recently detected by satellite-based instruments seem puzzling to researchers accustomed to thinking of thunderstorm discharges as driven by conventional air breakdown observed in the laboratory. However, the runaway air breakdown mechanism [*Gurevich et al.*, 1992; *Roussel-Dupré et al.*, 1994] produced by relativistic electrons with a mean energy of $\sim$1 MeV provides a natural solution to this dilemma. It also couples the γ-ray emissions to the high-altitude discharges [*Franz et al.*, 1990] recorded optically, recently termed blue jets and red sprites [*Franz et al.*, 1990; *Boeck et al.*, 1990; *Vaughan Jr. et al.*, 1992; *Lyons and Williams*, 1993; *Sentman and Wescott*, 1993; *Lyons*, 1994; *Sentman et al.*, 1995; *Wescott et al.*, 1995]. A very important advantage of this new breakdown mechanism is that the threshold electric field amplitude needed to initiate the process is a factor of approximately ten lower than the corresponding threshold for conventional breakdown. According to this new mechanism, breakdown is initiated by a high energy electron that is generated when a cosmic ray passes through the atmosphere. This energetic electron accelerates in the presence of strong thunderstorm electric fields, ionizes the air, and drives an avalanche process that leads to the formation of a relativistic electron beam with a mean energy of $\sim$1 MeV. Bremsstrahlung emissions caused by the beam interaction with the background air results in the production of large fluxes of γ-rays.

In this paper we present a detailed comprehensive model of red sprites and blue jets that yields optical and γ-ray results in excellent agreement with observation. Major results of this model were first presented at 1994 AGU Meeting in San Francisco [*Taranenko and Roussel-Dupré*, 1994].

The runaway breakdown mechanism used in our calculations is different from that suggested by *Chang and Price* [1995]. The *Chang and Price* [1995] mechanism is not feasible for two reasons: *i)* it has a threshold that is about twenty times larger than for the mechanism that we propose. The difference is due to the fact that in our mechanism discharge starts with several MeV electrons produced by cosmic ray secondaries whereas the Chang and Price model starts from cold electrons ("cold" runaway). *ii)* The electric fields required for "cold" runaway cannot be sustained in the medium due to regular air breakdown.

Paper number 95GL03502
0094-8534/96/95GL-03502$03.00

Theoretical Model of Runaway Air Breakdown

Runaway air breakdown was first suggested by *Gurevich et al.*, [1992]. A more detailed kinetic treatment [*Roussel-Dupré et al.*, 1994] describes the temporal evolution of the electron distribution function in a uniform background electric field. The spatial diffusion of the electron beam due to scattering was described in [*Gurevich et al.*, 1994]. The secondary (low energy) electrons are collision dominated and establish equilibrium distributions in time scales much shorter than the time of runaway breakdown. Their mean properties are derived from the standard swarm parameters [*Huxley and Crompton*, 1974]. The results are scaled in the usual way as a function of the applied electric field over pressure (E/p).

The present model uses the kinetic results for runaway electrons [*Roussel-Dupré et al.*, 1994] and applies the self-similar solution to a hydrodynamic model of upward discharges with varying electric fields. We model a discharge by evolving the mean properties of the two electron populations.

$$\frac{\partial n_p}{\partial t} = -\nabla(n_p\vec{v}_p) + \frac{1}{r}\frac{\partial}{\partial r'}(rD_\perp\frac{\partial n_p}{\partial r'}) + \frac{\partial}{\partial s}(D_\parallel\frac{\partial n_p}{\partial s}) + R_p n_p + \frac{F_c}{\lambda_{mfp}} \quad (1)$$

$$\frac{\partial n_s}{\partial t} = -\nabla(n_s\vec{v}_s) + R_s n_p - \alpha n_s - \alpha_R n_s n_+ + \alpha_D n_- + \nu_i n_s \quad (2)$$

$$\frac{\partial n_-}{\partial t} = \alpha n_s - \alpha_I n_- n_+ - \alpha_D n_- \quad (3)$$

$$\frac{\partial n_+}{\partial t} = R_s n_p + R_p n_p - \alpha_R n_s n_+ - \alpha_I n_- n_+ + \nu_i n_s \quad (4)$$

$$\frac{\partial q}{\partial t} = e\left[\nabla(n_p\vec{v}_p) + \nabla(n_s\vec{v}_s) - \frac{F_c}{\lambda_{mfp}}\right] \quad (5)$$

$$\nabla\vec{E} = 4\pi q \quad (6)$$

with $q = e(n_+ - n_- - n_s - n_p)$ and where n_p is the density of primary electrons (high energy runaway electrons), n_s is the density of secondary electrons, n_+ is the density of positive ions, n_- is the density of negative ions, r is the radial distance from the center of the discharge, r' is the spatial variable perpendicular to the local direction of the electric field, the longitudinal variable is oriented opposite to the local electric field, s is the spatial variable along the electric field, $D_\perp$, $D_\parallel$ are perpendicular and longitudinal diffusion coefficients, R_p is the production rate of runaway electrons, v_p is the mean primary electron velocity, F_c is the flux of cosmic-ray produced high-energy electrons, λ_{mfp} is the mean free path of high energy electrons with mean energy ϵ_p,

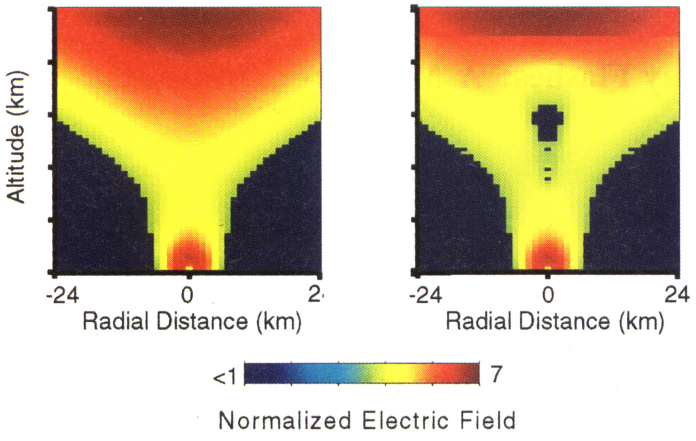

Figure 1. Ambient electric fields normalized to the local threshold amplitude [*Gurevich et al.*, 1992] of the runaway breakdown. (*a*)*Left*. The fields are established after the intracloud discharge. (*b*)*Right*. The fields are at 117 μs after initiation of the discharge by a single electron at 25 km.

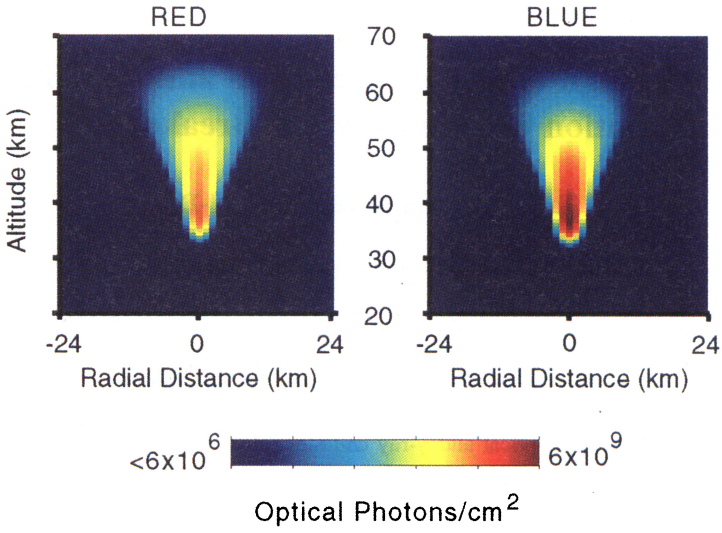

Figure 3. Space distribution of optical emissions integrated along horizontal lines of sight and over the duration of the discharge in the red (the 1-st positive band of N_2 400 nm to 500 nm) and the blue (the 2nd positive band of N_2 406.0 nm, 400 nm to 500 nm, and the 1-st negative band of N_2^+ 400 nm to 500 nm) parts of the optical spectrum.

$R_s = \frac{\epsilon_p}{\epsilon_i} R_p$ is the production rate of secondary electrons, $\epsilon_i = 34$ eV is the energy loss per ion pair produced in air, $\vec{v}_s$ is the mean velocity of secondary electrons, α is the three-body attachment rate, α_R is the recombination rate, α_D is the detachment rate, ν_i is the avalanche rate for low-energy electrons (ionization minus dissociative attachment), and α_I is the ion recombination rate. The parameters ϵ_p, $\vec{v}_p$ and R_p are available as a function of E/p from the detailed kinetic calculations (including the effect of the geomagnetic field) while $\vec{v}_s$, $\alpha, \alpha_R, \alpha_D$, and ν_i are available as a function of E/p from the literature (e.g. [*Huxley and Crompton*, 1974; *Ali*, 1986]). The flux F_c of high-energy secondary electrons is also available from the literature (e.g.[*Daniel and Stephens*, 1974]) and the mean free path λ_{mfp} is well defined in terms of Bethe's energy loss formula. Note that we have assumed that the heavy ions are effectively stationary over the development of the

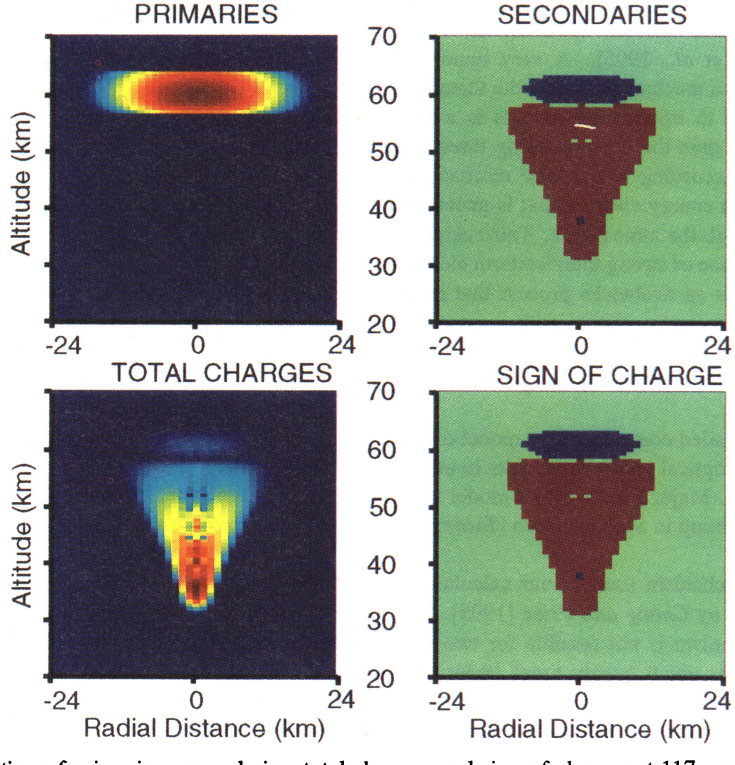

Figure 2. Distribution of primaries, secondaries, total charges, and sign of charges at 117 μs after initiation of the discharge by a single electron at 25 km. The brown represents maximum values which are 0.35 cm^{-3}, 4.17 x 10^4 cm^{-3}, and 113 cm^{-3} and the dark blue represents minimum values which are less than 3.5 x 10^{-4} cm^{-3}, 41.7 cm^{-3}, and 0.113 cm^{-3} for number of primaries, secondaries, and total charges respectively. For the polarity of charge the brown represents positive charge, the dark blue represents negative charge, and the green is close to neutral.

discharge, i.e. v_+ and v_- are zero. Eqs. (1)-(6) are used to evolve for the electron and ion densities as well as the electrostatic field vector E that allows us to determine $\vec{v}_s$ and $\vec{v}_p$.

Establishment of Driving Electric Fields.

Large amplitude electric fields in the upper atmosphere can be established after an intracloud discharge [e.g., *Dejnakarintra and Park*, 1974; *Baginski et al.*, 1988] annihilating positive charge distributed at the cloud tops (e.g., 15 km altitude) and negative charge at the cloud bottoms (e.g., 5 km altitude). The results of a model calculation for the electric field configuration following such a discharge is shown in Fig. 1a. Our model assumes that 100 C of charge are established by slow (time scale of tens of seconds) charge separation processes in the cloud. Solving Poisson's equation and the charge continuity equation in the conductive atmosphere with the specific conductivity profile [*Dejnakarintra and Park*, 1974] we find that polarization charges above the clouds are attracted to the cloud resulting in shielding of the upper atmosphere from the cloud electric fields. Simulating an intracloud discharge, we remove 90% of the cloud charges in 5 ms. The polarization charges above the clouds respond at a much slower rate, resulting in the penetration of quasi-static electric fields to high altitudes as shown in Fig. 1a. The evolution of electric fields in the upper atmosphere occurs at ms or longer time scales. Whereas MeV electrons move with a velocity close to the speed of light and pass the upper atmosphere in ~200 μs. Hence, we consider ambient electric fields as constant during runaway air breakdown in the upper atmosphere.

Model of the Discharge.

We stimulate the initiation of the runaway air breakdown by injecting a single MeV electron produced by a cosmic ray at 25 km altitude. At the beginning of the discharge the beam of primary electrons is weak and we can neglect the electric fields produced by charged particles separated in the discharge itself in comparison to the ambient electric fields. However, if the length of the region occupied by strong electric fields allows, the discharge grows in size and the electric field produced by separating primary and secondary electrons from positive ions becomes comparable to the amplitude, and opposite to the direction of the driving ambient field. This process prevents further growth of the beam. At this stage of the discharge a self-consistent solution of eqs. (1)-(6) is required. We numerically solve these equations assuming cylindrical symmetry.

An example of the field amplitude at the developed stage of the discharge is shown in Fig. 1b. The corresponding distribution of primary and secondary electrons, total charges, and sign of charges, as obtained from solution of equations (1)-(6), is shown in Fig. 2. The distribution of charges makes it clear that the electric field inside the region of the discharge must be decreased in comparison to the ambient. In the present simulation the local directions of the propagation of electrons are assumed to coincide with the direction of the local ambient electric field. Changing the amplitude of the electric field is expected to be more important than changing its direction due to the discharge simply because it is the strength of the field that determines the production rates of extra ionization, x-ray, γ-ray, and optical emissions. The present simplification underestimates the perpendicular diffusion rate of the beam. However this approximation is not expected to change the qualitative dynamics of the discharge. The approximation of a quasi-constant electric field is valid as long as the fields do not substantially change during the characteristic time interval for an avalanche to occur. This approximation allows us to use hydrodynamic coefficients obtained under assumption of constant fields. The important thing is not just the absolute value of the electric field but its value normalized to the local breakdown threshold. The ambient normalized electric field varies from two to seven over 40 km in altitude which means that the normalized gradient is small indeed. During the breakdown fields cannot be changed on the time scale shorter than the avalanche time simply because the avalanche time determines the rate of charge supply.

trations of ions. At high altitudes their intensity is lower than the intensity of emissions generated by electron impacts. Hence, at video rates, high altitude parts of the flashes are formed due to electron impacts and appear predominantly at a single frame whereas at low altitudes the images are formed by emissions from recombinating ions and as such are seen on several frames. The combination of the two types of emissions with their altitude dependent duration can produced a visual effect of motion of the discharge with a velocity that is different from the velocity of primary electrons. Another explanation for the observed velocity [*Wescott et al.*, 1995] of blue jets lies in the development of the source electric field configuration. However its details are left for further publication.

Computed Optical Emissions.

We compute the spatial distribution of the optical emissions resulting from direct electron impact, which we will term "primary emissions", using the air fluorescence efficiencies [*Davidson and O'Neil*, 1964; *Mitchell*, 1970]. The results for the red (the 1-st positive band of N_2 400 nm to 500 nm) and blue (the 2nd positive band of N_2 406.0 nm, 400 nm to 500 nm, and the 1-st negative band of N_2^+ from 400 nm to 500 nm) regions of the spectrum are shown in Fig. 3. It is seen that the blue emissions dominate at low (< 50 km) altitudes (by a factor of up to ten) while the red emissions dominate at high altitudes (by a factor of up to three). The number of photons shown in Fig. 3 is the upper limit of the brightness of upward discharges for a given value of the electric field since the discharge was initiated at a low altitude that gave enough space for its development. Discharges initiated at higher altitudes will generate lower intensities. The absolute number of photons in Fig. 3 ($\sim 10^{10}$ ph/cm^2) corresponds to intensity of one mega-Rayleigh for ~10 ms integration time which coincides with the latest estimates of the maximum intensity of the discharges for the brightest events [*Sentman et al.*, 1995; *Wescot et al.*, 1995].

Primary emissions shown in Fig. 3 appear within < 6μs which is determined by the natural lifetime of the excited states, following the passage of the primary electron beam which propagates through at a speed close to that of light. If we have an emitting region with an altitude extent H and a horizontal extent L then emissions are excited for a time interval $t_e = H/c$ (where c is the speed of light), and last an additional time period $t_a = L/c$. For H = 30 km and L = 10 km, we find t_e = 0.1 ms and t_a = 0.033 ms. Hence, the duration of primary emissions is shorter than 1/60 s which is the integration time of a typical video camera.

Recombination of positive and negative ions is another source of optical emissions. A detailed calculation of these emissions is beyond the scope of this work, however, we estimate their intensity and duration. We find that at 40 km the intensity is comparable to intensity of optical emissions produced by electron impacts and the duration is ~300 ms. Such emissions can explain long (from tens to hundreds of ms) duration of optical emissions at low altitudes with high ($N_i > 10^6$ cm^{-3}) concen-

Computed Gamma-Ray Emissions.

The time dependence of the 100 keV γ-ray flux at 500 km from the source was calculated using the efficiencies for γ-ray generation provided in [*Roussel-Dupré et al.,* 1994] and the same solution of eqs (1)-(6). In these calculations, we assumed that the photons are neither absorbed nor scattered in the atmosphere. Under such approximations, a detector of area 2000 cm^2 having 100% efficiency is expected to register ~800 counts per burst. The hardness of the spectrum corresponds to Bremsstrahlung emissions generated by ~1 MeV primary electrons. Both of these results are in a very good agreement with recent observations *Fishman et al.,* 1994]. Due to absorption in the upper atmosphere the total number of γ-ray photons registered at the satellite should be smaller than that predicted here by perhaps as much as a factor of three. Diffusion of the photons in the atmosphere can extend duration of a single burst observed at the satellite by several hundred μs, a combination of several discharges occurring above the same cloud complex could extend the total duration of an event up to from tens to hundreds of ms.

Discussion.

We establish that: *i)* the runaway discharge model predicts the altitude range, shape, velocity of visual appearance, intensity and spectra of optical emissions observed in upward discharges, and *ii)* relates the upward discharges to γ-rays of atmospheric origin giving the correct hardness and number of counts. It is evident from Fig. 2 that the lowest relative value of the field occurs at an altitude of ~40 km. This is the region where a discharge originated at lower altitudes can be most easily interrupted when, for example, ambient fields are established by a weaker tropospheric discharge than the one considered in this example. Hence such a region of relatively low fields separates blue jets from red sprites as observed in most of the optical data.

In comparing the present model to models attempting to explain the phenomenon of upward discharges based on a regular type of air breakdown [*Taranenko et al.,* 1993 a,b; *Pasko et al.,* 1995; *Milikh et al.,* 1995; *Rowland et al.,* 1995], we note that the present one most easily reproduces the shape of the discharge (elongated in the vertical direction), requires smaller field values, covers the complete altitude range and relates the upward discharges to observation of γ-rays.

Acknowledgments. We thank Bill Feldman of Los Alamos National Laboratory for valuable comments on the manuscript and Earl Williams of the Massachusetts Institute of Technology for a fruitful discussion on penetration to the mesosphere of electric fields from tropospheric lightning. The work was performed under the auspices of the Department of Energy and supported in part by the Commissariat a l'Energie Atomique, Laboratoire de Detection et de Geophysique, France.

References

Ali, A.W., Intense and short electric field (dc and microwave) Air-Breakdown Parameters, NRL Memorandum Report, 5815, 1986.

Baginski, M. E., L. C. Hale, and J. J. Olivero, Lightning-related fields in the ionosphere, *Geophys. Res. Lett., 15,* 764, 1988.

Boeck, W.L., Vaughan, Jr., O.H., and Blakeslee, R.J., Low light level television images of terrestrial lightning as viewed from space, *EOS Trans. AGU, 72,* 171, 1990.

Chang, B., and C. Price, Can gamma radiation be produced in the electrical environment above thunderstorms?, *Geophys. Res. Lett., 22,* 1117, 1995.

Daniel, R.R., and S.A. Stephens, Cosmic-ray-produced electrons and gamma rays in the atmosphere, *Rev. Geophys. 12,* 233, 1974.

Davidson, G., and R. O'Neil, Optical radiation from nitrogen and air at high pressure excited by energetic electrons, *J. Chem. Phys. 41,* 3946, 1964.

Dejnakarintra, M., and C. G. Park, Lightning-induced electric fields in the ionosphere, *J. Geophys. Res., 79,* 1903, 1974.

Fishman, G.J., Bhat, P.N., Mallozzi, R., Horack, J.M., Koshut, T., Kouveliotou, C., Pendleton, G.N., Meegan, C.A., Wilson, R.B., Paciesas, W.S., Goodman, S.J., Christian, H.J., Discovery of intense gamma-ray flashes of atmospheric origin, *Science 264,* 1313, 1994.

Franz, R.C., Nemzek, R.J., and Winckler, J.R., Television image of a large upward electrical discharge above a thunderstorm system, *Science 249,* 48, 1990.

Gurevich, A.V., Milikh, G.M., and Roussel-Dupré, R.A., Runaway electron mechanism of air breakdown and preconditioning during a thunderstorm, *Phys. Lett. A, 165,* 463, 1992.

Gurevich, A. V., G. M. Milikh, and R. A. Roussel-Dupré, Nonuniform runaway air-breakdown, *Phys. Lett. A, 187,* 197, 1994.

Huxley, L.G.H., and R.W. Crompton, The diffusion and drift of electrons in gases, Wiley Series in Plasma Physics, (John Wiley & Sons, New York), 1974.

Lyons, W. A., and Williams, E. R., Preliminary investigations of the phenomenology of cloud to stratospheric lightning discharges, *17-th Conference on Severe Local Storms & Atmospheric Electricity, American Meteorological Society,* Oct. 4-8, 1993, St. Louis MO , 1993.

Lyons, W.A., Characteristics of luminous structures in the stratosphere above thunderstorms as imaged by low-light video, *Geophys. Res. Lett., 21,* 875, 1994.

Milikh, G. M., K. Papadopoulos, and C. L. Chang, On the physics of high altitude lightning, *Geophys. Res. Lett., 22,* 85, 1995.

Mitchell, K.B., Fluorescence efficiencies and collisionl deactivation rates for N_2 and N_2^+ bands excited by soft X rays, *J. Chem. Phys. 53,* 1795, 1970.

Pasko, V.P., U. S. Inan, Y. N. Taranenko, and T. F. Bell, Heating, ionization, and upward discharges in the mesosphere due to intense quasi-electrostatic thundercloud fields, *Geophys. Res. Lett., 22,* 365, 1995.

Roussel-Dupré, R.A., Gurevich, A.V., Tunnell, T., and Milikh, G.M., Kinetic theory of runaway air breakdown, *Phys. Rev. E, 49,* 2257, 1994.

Rowland, H. L., R. F. Fernsler, J. D. Huba, and P. A. Bernhardt, Lightning driven EMP in the upper atmosphere, *Geophys. Res. Lett., 22,* 361, 1995.

Sentman, D.D., and Wescott, E.M., Observations of upper atmospheric optical flashes recorded from an aircraft, *Geophys. Res. Lett., 20,* 2857, 1993.

Sentman, D.D., E.M. Wescott, D.L. Osborne, D.L. Hampton, and M.J. Heavner, Preliminary results from the Sprites94 aircraft campaign: red sprites, *Geophys. Res. Lett., 22,* 1209,1995.

Taranenko, Y.N., Inan, U.S., and Bell, T.F., Interaction with the lower ionosphere of electromagnetic pulses from lightning: heating, attachment and ionization, *Geophys. Res. Lett., 20,* 1539, 1993 a.

Taranenko, Y.N., Inan, U.S., and Bell, T.F., Interaction with the lower ionosphere of electromagnetic pulses from lightning: excitation of optical emissions, *Geophys. Res. Lett., 20,* 2675, 1993 b.

Taranenko, Y. N. and R. Roussel-Dupré, AGU Fall Meeting, Dec. 5-9, San Francisco, California, 1994.

Vaughan, Jr., O.H., Blakeslee, R.J., Boeck, W.L., Vonnegut, B., Brook, M., and McKune, Jr., J., A cloud-to-space lightning as recorded by the space shuttle payload-bay TV cameras, *Monthly Weather Review, 120,* 1459, 1992.

Wescott, E.M., D. Sentman, D. Osborne, D. Hampton, and M. Heavner, Preliminary results from the Sprites94 aircraft campaign: blue jets, *Geophys. Res. Lett., 22,* 1213,1995.

Yuri Taranenko and Robert Roussel-Dupré, Los Alamos National Laboratory, Los Alamos, NM 87545.

(Received: April 24, 1995; revised: October 16, 1995
accepted: October 19, 1995)